Third United Nations International Conference on the Peaceful Uses of Atomic Energy

A/CONF.28/P/366
USSR
May 1964
Original: RUSSIAN

Confidential until official release during Conference

NEUTRON THERMALIZATION STUDIES IN HYDROGENOUS MEDIA

Doilnitsyn Ye.Ya., Novikov A.G., Ilyasova G.A., Panarin M.V., Smelov V.V., Stakhanov I.P., Stepanov A.S., Stupak A.I.

At present the most important hydrogenous neutron moderating materials in reactor technics are water and some metal hydrides.

When neutrons are thermalized in water the effects of atomic chemical binding and of the molecular diffusion of liquid are revealed.

When neutrons are moderated in metal hydrides energy exchange between a neutron and moderator goes on by portions defined by the oscillation levels of a proton which is rigidly bound with metal atoms in a lattice. The total cross-section of metal hydrides exhibits large effect due to rigid binding of a proton with metal atoms in a lattice[I].

To reveal some peculiarities in forming thermal neutron spectra in these media the experiments on neutron thermalization in water and lithium-7 hydride were performed and the total cross-sections of lithium-7 hydride, zirconium hydrides with different H-content were measured. Experimental results are compared to calculations taking into account specific features of the moderators studied.

I. Neutron Thermalization in Water and Boric Acid Solutions

When studying neutron thermalization in water the following problems were considered:

I) The process of thermal neutron spectrum forming at different distances from a source was studied.

2) Relaxation length of neutron gas temperature was found directly from experiment and the effects observed were compared with calculations for the given experimental con-

ditions.

3) Absorber concentration influence on thermal neutron spectrum forming in infinite medium with uniformly distributed sources was studied by the comparison of experimental results with calculations performed with a model taking into account chemical binding strength[2],[3].

Experimental data necessary to solve the above mentioned problems were obtained by means of space-energy distribution measurements of thermal neutrons in water produced by spherical source with its spectrum being in one case nearly Fermi-distribution and in the second case-Maxwellian distribution with $T = 760^{\circ}K$.

§ I. Experimental Method

Thermal neutron spectra in water at different distances from the source were measured by time-of-flight method.

The arrangement used for these purposes is shown in Fig.I.

Cylindrical tank with 500 mm in diameter and 600 mm high mounted near the graphite-water power reactor shielding was filled with distilled water. Collimated neutron beam passed through the cylindrical tube (d = 30 mm) onto the lead sphere (r_0 = 20 mm) placed in the centre of the tank filled with water. This sphere isotropically scattering the incident neutrons imitated approximately a spherical source. Beam hole placed at 70° to the primary beam direction was a tube of rectangular cross-section I5x30mm.

Thermal neutron beam distribution around the sphere measured by indium indicator activation only in the direct direction had some assymmetry (~20%) which disappeared already completely in the region of the beam hole.

Neutron spectra, set up in water, were studied by means of the mechanical selector which was described in[4]. The energy resolution in these measurements was $\simeq 40 \mu sec./m$.

Beam hole, mechanical chopper and detector being fixed relative to one another, they were able to move along the beam hole direction that permitted to measure spectra in water at different distances from the sphere. The data obtained by means of indium indicators were used for the normalization of neutron spectra according to their amplitudes and for the introduction of a correction on the gradient effect.

In all the figures the neutron spectra are represented as : $\frac{dn}{dt} = N(t)$

where $\frac{dn}{dt}$ - neutron density in the unit interval of time-of-flight;

t - time-of-flight in $\mu sec./m$.

Source spectrum, i.e. the spectrum of neutrons scattered by the sphere, measured without water in the tank, is shown in Fig.2.

In water the measurements were carried out at the following distances from the sphere: $r - r_0 = 0$; 10mm; 20mm; 50mm; 65mm (r - the distance from the sphere centre to the point investigated). At each of these distances the spectrum was measured twice: without Cd and with Cd placed at the beam inlet to the tank. Experimental curves taken with Cd in the primary beam represent neutron spectrum from the source with Fermi distribution, as it is seen from Fig.2. Experimental curves $N(t)$ for the given distance as the difference between two measurements (without Cd and with Cd in the primary beam) represent neutron spectrum in water caused by the thermal component of the reactor beam which (as it is seen from Fig.2) is nearly Maxwellian with $T_H = 760^{\circ}K$.

§ 2. Thermal Neutron Spectra from the Source with Fermi Distribution

Space-energy neutron distribution from the source with Fermi spectrum is shown in Fig.3. In all the points studied (including the measurements close to the sphere) thermal

range of the spectra is satisfactorily described by Maxwellian distributions at temperatures slightly exceeding the temperature of the medium and coinciding within experimental errors.

The results of this experiment are compared with the calculation of the thermal neutron space-energy distribution in water carried out for spherical geometry. The calculation was performed in P_1-approximation in the energy range $0 < E < 0.67$ ev divided into I5 groups. Thermalization effects were accounted for on the basis of the work by Turchin V.F. 5 . At $E > 0.67$ ev (source region) the neutron spectrum was assumed to be a Fermian one. Experimental curve obtained with the help of sodium indicators ($E = I.46$ev) was used as spatial distribution of the source. The details of the method used in this calculation may be found in [3], [5] .

Experimental and calculational curves were normalized according to distribution maximum $N(t)$.

From Fig.3 the results of experiment and calculation are seen to agree sufficiently well. Calculational curves practically coincide with the corresponding Maxwellian distributions in thermal regions. Therefore both experimental and calculational data allow to make a conclusion that with Fermian spectrum source thermal neutron energy distribution in water(in the range $E \leqslant 0.I5$ev) does not depend on the distance to the source and can be described at any point of the medium by the thermal neutron spectrum for infinite medium with distributed sources [3] (accurate within a small correction on the localized neutron leakage, § 4).

§ 3. Thermal Neutron Spectra from the Source with Maxwellian Distribution Temperature 760°K.

Space -energy neutron distribution in water created by the source with the spectrum being a thermal component of the reactor beam (difference curves) is shown in Fig.4.

Experimental curves were determined to be close to Maxwellian distribution at $r - r_0 \geq 20$ with temperature $T_H = 304^\circ K$ (the temperature averaged over the measurements at three distances: 20 mm- $303 \pm 15^\circ K$; 50mm- $306 \pm 15^\circ K$; 65 mm- $302 \pm 15^\circ K$). Therefore to begin with the distance ~20 mm from the sphere the spectrum of this source does not influence the neutron energy distribution within experimental accuracy.

In the range $r - r_0 < 20$ mm which may be called a transitional one the neutron distributions measured are of essentially different character. These curves were compared with the calculation based on the assumption that the process of setting up medium spectrum goes through Maxwellian-like forms with the temperature depending on the distance to the source. Kinetic equation was solved by Grad method [6] by Ermit symmetrized polynomial expansion of the neutron distribution function. Expansion parameter, neutron temperature T, was chosen so that the distribution function was sufficiently well approximated by the first two members:

$$T = \frac{m}{3kn} S_\rho J_{ik} \qquad (I)$$

where J_{ik} is the second moment of the distribution function.

By integration of kinetic equation over the velocity space we get the system of equations for T, n (neutron density) and $\vec{J}$ (neutron current):

$$\begin{aligned} &\frac{\partial n}{\partial t} + \frac{\partial J}{\partial x_i} + \gamma n = 0; \\ &\frac{\partial nT}{\partial t} + \frac{5}{3}\frac{\partial}{\partial x_i} n J_i + \gamma n T = \frac{T - T'}{T'} n T \frac{1}{\tau}; \qquad (2) \\ &J_i = -\frac{k}{m}\frac{1}{\lambda}\frac{\partial nT}{\partial x_i}; \end{aligned}$$

where T' - medium temperature, γ - absorption coefficient, m - neutron mass.

Kinetic coefficients λ and τ were determined in the following way:

$$\lambda = \frac{4}{3}\frac{1}{\sqrt{\pi}} n' \frac{1}{\beta} \int dx\, d x' e^{-x^2} \left[\sigma(x' \to x) x'^5 - \sigma_1(x' \to x) x x'^4 \right];$$

366

$$\frac{1}{\tau} = \frac{2}{3}\frac{1}{\sqrt{\pi}} n' \frac{1}{\beta} \int dx\, dx' e^{-x'^2} (x^2 - x'^2) x'^3 \sigma_0 (x' \to x); \quad (3)$$

where n' - medium molecule density, x - dimensionless velocity ($x = \beta v$; $\beta^2 = \frac{m}{2kT}$), σ_0 and σ_1 - zero and the first moments of the scattering indicatrix.

The solution of system (2) for a stationary case without absorption and spherical source with temperature T_0 gives [4] :

$$|T' - T| = |T' - T_0| \exp\left\{-\frac{1}{L^2}\left[\frac{r^2 - r_0^2}{2} + \frac{r^3 - r_0^3}{3R}\right]\right\} \quad (4)$$

where r_0 - source radius, R - radius characterizing the total system dimensions; $L = \left(\frac{5}{3}\frac{\tau}{\lambda}\frac{kT'}{m}\right)^{1/2}$ ✱ relaxation length of neutron gas temperature.

To compare experimental data with this calculation the difference curves $N(t)$ obtained at different distances from the sphere were to be approximated by Maxwellian distributions. Their temperature was selected so as to achieve the best coincidence of Maxwellian distribution with the right slope of the corresponding difference curve. This method of the determination of the temperatures is based on the assumption that if the current of "hot" source neutrons results in distribution function anisotropy then the right slope of the experimental curve is a region of the spectrum where this anisotropy is pronounced most weakly. Neutron temperatures thus found proved to be equal to: for $r - r_0 = 0$, $T = 500 \pm 30^\circ$K;

✱ For the case of flat problem without absorption neutron temperature distribution becomes

$$|T' - T| = |T' - T_0| \exp\left\{-\frac{x}{L_x}\right\}$$

L_x is related with the obtained above relaxation length by the following relation:

$$L^2 = L_x a,$$

where a is the value characterizing the system size. In the presence of absorption a depends on the diffusion length.

366

for $z - z_0 = 5$ mm, $T = 360 \pm 20^\circ K$; for $z - z_0 = 10$ mm, $T = 317 \pm 15^\circ K$ (Fig.5). Using the expression (4) and the temperatures obtained for different distances it was found that $L = 1 \pm 0.2$ cm . Neutron temperature relaxation length calculation on the basis of the model proposed in [2] gives for our case $L = 1.1$ cm . The dependence of neutron temperature on the distance to the sphere calculated according to (4) with $L = 1$ cm is shown in Fig.5 .

From Fig.4 it follows that difference curve approximation by Maxwellian distributions may be considered to be satisfactory at the distances where the spectrum becomes nearly asymptotic one but this approximation is not valid for the region where the source proximity causes the marked distribution function anisotropy. A more precise description of the experimental curve shape over the whole transient region may be obtained by representing these curves as superposition of source spectrum (Maxwellian distribution with $T = 750^\circ K$) and of asymptotic medium spectrum(Maxwellian distribution with $T = 300^\circ K$) with the amplitudes depending on the coordinates.Similar approach was already repeatedly used in a number of calculational and experimental works, for example, in [7] ,[8] . Difference curve expansion in two such components is shown in Fig.6.

Spectrum character at energies ~ 0.01 ev was assumed to be completely defined by Maxwellian distribution with $T = 300^\circ K$. So asymptotic components proved to be found. By subtracting them from difference spectra the curves similar in shape to Maxwellian distribution with $T = 750^\circ K$ but with different amplitudes were obtained for all the three distances (0.5mm and 10mm).
Densities of the "hot" and "cold" components found as a result of this expansion as functions of the distance from the source are presented in Fig.7 .

An attempt to obtain similar curves by calculation was made . Neutron distribution function was represented

as the superposition of two components each of which depended only on one of the temperatures. The calculation method used did not differ much from the above mentioned one.

The calculation was performed for two cases: for the medium without absorption and with slight absorption. From Fig.7 which represents the comparison of these calculations with experiment it is difficult to give preference to any of the calculation curves. At great distances, however, experimental points for"cold" neutron density are nearer to the calculation data taking into account the absorption.

§ 4. Neutron Spectra in Boric Acid Solutions

When measuring thermal neutron spectra in boric acid solutions the experimental arrangement described above was used. Neutron flux from the reactor at the tank inlet was always covered with cadmium, and the butt-end of the beam tube was placed above the sphere that resulted in small gradient of scalar flux in the direction of beam direction.

When comparing the results obtained by the calculations for infinite medium with uniformly distributed sources it is necessary to introduce a correction for the local diffusion neutron leakage. In the region near the source this correction at first sight seems to be considerable. However, the distribution type of neutron flux created by our source spectrum is such that beam extraction region ($\tau - \tau_0 \approx$ Icm) is close to the bend point of the curve describing the distribution of this flux. Local leakage is revealed here as slight additional absorption($\frac{\nabla^2 \phi}{\phi} < 0$) accounting for ~ I5% from the total absorption for pure water and practically does not affect the experimental results with additional absorber.

Experimental results [9] and their comparison with calculations performed for infinite medium with uniformly

distributed sources [3] are presented in Fig.8. When plotting the data T_H/T_0 as a function of absorber concentration, additional absorption caused by local diffusion leakage is accounted for. In internal region experimental curves satisfactorily agree with calculation spectra which prove to be nearly Maxwellian distributions with temperatures shown in the same figure. T_H/T_0 values as a function of absorber concentration in water are compared in Fig.9 with calculations performed in 2 3 with accounting for chemical binding forces (curves I and 2) and according to the gas model(curve3).

It must be pointed out that the results of the last calculations described in the paper presented to the present conference [2] agree better with our data.

The whole set of the experimental values T_H/T_0 cannot be explained on the basis of gas model.

II. The Study of Neutron Hydride Moderating Properties

§ I. Total Cross-Sections of Lithium-7 and Zirconium Hydrides

Total cross-sections of metal hydrides were measured by means of mechanical neutron selector described in [I0] [II]. Spindle-shaped slits in the rotor and the system of syncronously rotating rotors ensured negligible background in the measurements at flight path I30 m with resolution 3 μsec/m in thermal region.

Figure I0 shows the trend of the total cross-section curve for the neutrons scattered by hydrogen bound in lithium-7 hydride according to the data of measurements of lithium-7 hydride total cross-section from 0.02 ev to 2 ev.

At neutron energy above 0.2 ev scattering cross-section obtained experimentally follows the law [I2] [I3] :

$$\sigma_s(E) = \sigma_0\left(1 + \frac{k_v}{3\mu E}\right) \qquad (5)$$

where k_v -average proton kinetic energy, μ - proton mass to neutron mass ratio, σ_0 - cross-section of scattering by a free nucleus.

Calculational cross-section values for neutron scatter-

ing by litium-7 hydride obtained in [2] with regard for levels at 0.I ev, 0.I3 ev and acustic oscillations satisfactorily agree with experimental data. In Fig.IO the dotted curve represents the calculated values in the range of 0.I ev level where there is a slight difference as compared to the experimental results. Good agreement between experimental and calculational data is observed in all the rest of the range. Zirconium hydride total cross-section was measured for zirconium hydrides with different "H" content: $Zr H_{0.8}$; $Zr H_{1.5}$; $Zr H_2$. The results of the measurements show the agreement between the total cross-sections of zirconium hydrides within experimental accuracy (4%) and with the data published in [I].

No displacement of oscillation levels of H in the lattice was observed for zirconium hydrides with different H - content.

Neutron scattering cross-section in the range $E > 0.5$ ev is described by the relation (5).

§ 2. Neutron Thermalization in Lithium-7 Hydride

Neutron thermalization in lithium-7 hydride was studied by the method described above in this report(§4). The same arrangement, identical geometry and similar methods of experimental data analysis were used in these experiments. An assembly from lithium-7 hydride had cylindrical form with d =430 mm and H = 520 mm out of disks with d = 47mm and H =5mm. Disks from hydride (canned with aluminium 0.I mm thick) were packed up so as to reduce the escape of neutrons through the assembly slits (in every hydride layer the disks are displaced so as to prevent neutron leakage without moderation)· The lead sphere (d -50mm) is placed in the centre of the assembly. Neutron beam from the reactor went through the reentrant hole (of square cross-section with side =35mm) onto the lead sphere. Cadmium was placed on its way before the assembly. Neutron beam went out from the hole butt-end above the

sphere centre. Extraction tube was of rectangular cross-section 20x35 mm .

The results of measurements of thermal neutron density are given in Fig.II a s a function of time-of flight in $\mu sec./m$. Statistical accuracy of $\frac{dn}{dt}$ determination was 3%.

To a first approximation thermal neutron spectrum in lithium-7 hydride may be described by Maxwellian distribution with temperature $T = 330^{\circ} \pm 10^{\circ}K$. The comparison of these results with corresponding spectrum measurements in water, at the same temperature and with equal absorption per hydrogen atom shows the neutron spectrum setting up in lithium-7 hydride to be more hard than that in water. To evaluate more obviously the hardness of the spectrum obtained in lithium-7 hydride, Fig.I2 shows the ratio $T_{\mu}/T_{\circ}$ obtained for lithium-7 hydride and the calculational data for water [2] . In the same figure calculation curve for lithium-7 hydride taken from the same work is presented. Neutron absorption for lithium-7 hydride plotted on the abscissa axis takes into account the effective cross-section of impurity Li^6. From figure I2 good agreement between experimental data and calculated data obtained in [2] is seen.

The comparison of $T_{\mu}/T_{\circ}$ for lithium-7 hydride and water reveals that thermal neutron spectrum setting up in hydride is close to the spectrum in water poisoned by absorber according to $1/v$ law with absorption in water being nearly twice the absorption in lithium hydride. Thermal neutron spectrum in lithium-7 hydride is softer as compared to neutron distribution setting up in zirconium hydride at the same absorption.

CONCLUSION

The experiments on the studies of the moderating properties of water, lithium-7 and zirconium hydrides and their comparison with calculations show the experimentally observed effects to agree well enough with the calculations performed with the corresponding differential cross-sections in [2].

REFERENCES

I. Mc Reynolds A.W., Nelkin M., Rosenbluth M., Whittemor W., Second Geneva Conference, I958, Report No I540.

2. Mayorov L.V., Turchin V.F., Yudkevitch M.S., " Chemical Bond Influence on Neutron Thermalization" Report presented to the 3d International Conference on the Peaceful Uses of Atomic Energy, Geneva, I964.

3. Marchuk G.I., Turchin V.F., Smelov V.V., Ilyasova G.A Atomnaya Energiya, I3, 534, I962.

4. Doilnitsyn Ye.Ya., Novikov A.G., Stakhanov I.P., Stepanov A.S. , Atomnaya Energiya, I5, 255, I963.

5. Turchin V.F., "Inelastic Scattering of Neutrons in Solid and Liquids" , International Atomic Energy Agency , Vienna , 259, I96I

6. Grad A. Communs.pure and appl.math. 2, 23I, I949.

7. Selengut D.S., Nucl.Sci.and Eng. 9, I, 94, I96I.

8. Bennet R.,Neinman R., Nucl.Sci.and Eng. 8, 4, I960.

9. Doilnitsyn Ye.Ya., Novikov A.G., Atomnaya Energiya, I3, 49I, I962.

I0. Vladimirskii V.V., Sokolovskii V.V., 2d International Conference on Peaceful Uses of Atomic Energy, Report 204I, Geneva, I958.

II. Doilnitsyn Ye.Ya., Hamyanov L.P., Klemyshev P.S., Materials of Symposium on Slow Neutron Physics. Dubna , I93, I962.

I2. Placzek I., Phys.Rev. 86, 377, I952.

I3. Messian F.A., Journal de physique et le radium, I2, No 6, 670, I95I.

I4. Walton R.B., Beyster J.R., Wood J.L., Lopez W.M., Nucl.Sci.and Eng., 9, I96I.

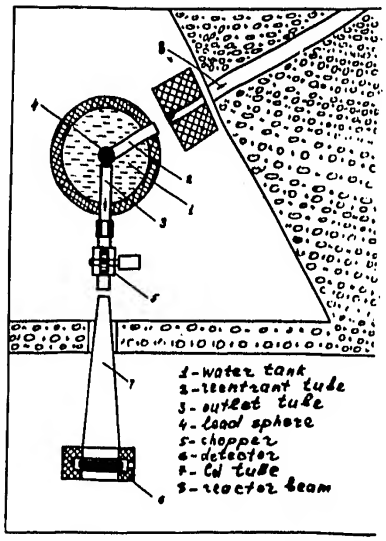

Fig.I. Experimental arrangement diagram.

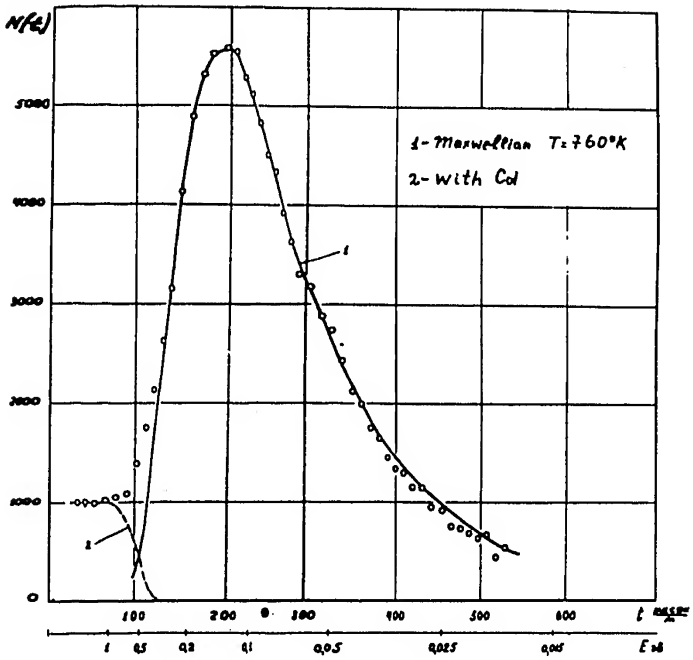

Fig.2. Source spectrum.

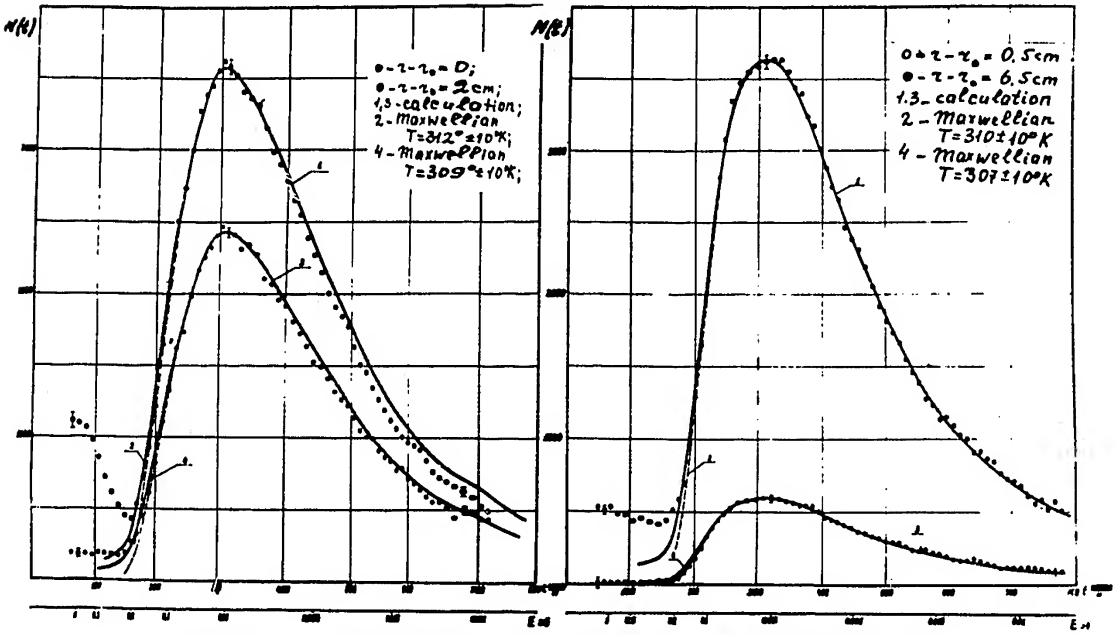

Fig.3. Neutron spectra at different distances from the source with Fermi distribution.

366

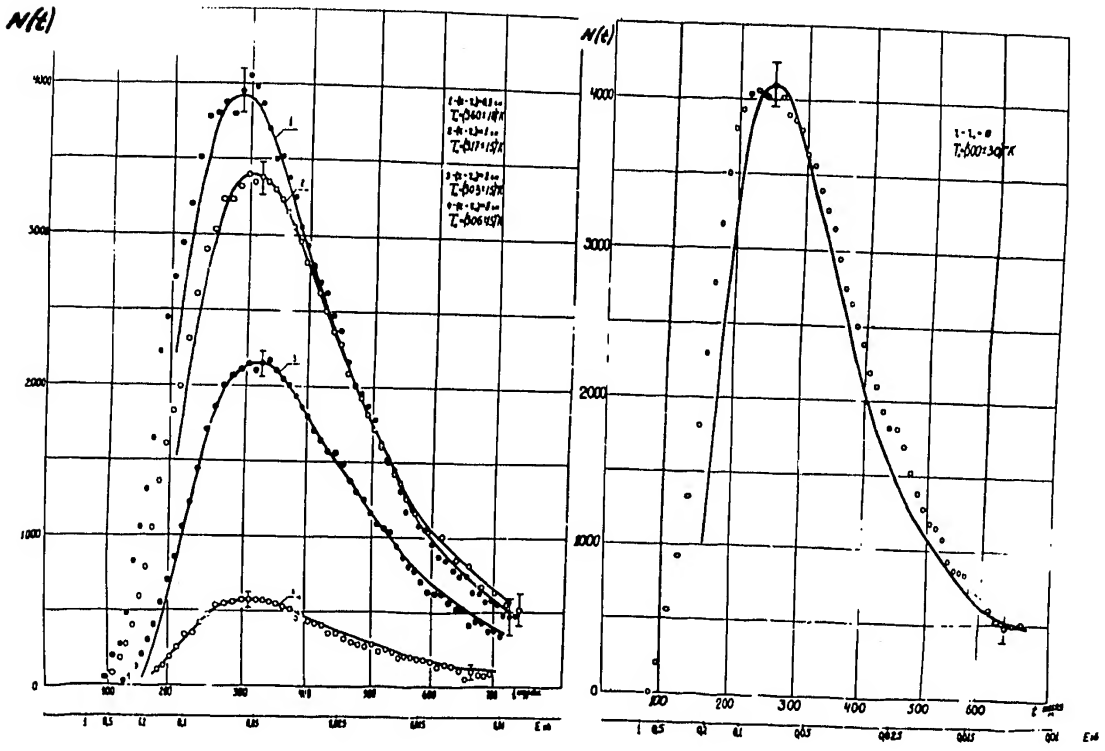

Fig.4. Difference spectra at different distances from the source.

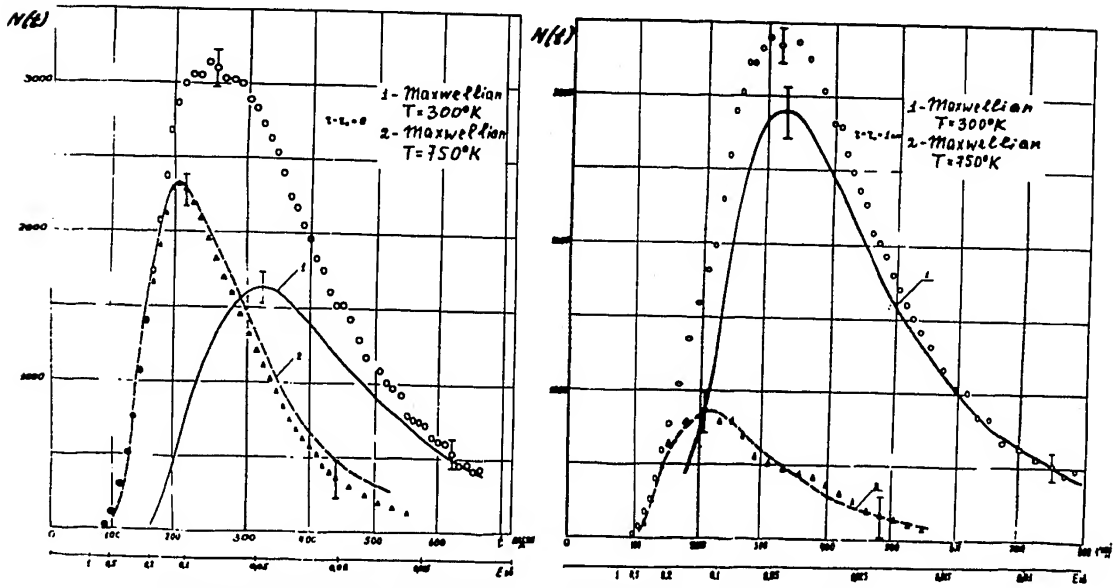

Fig.6. Difference spectrum expansion into two components

366

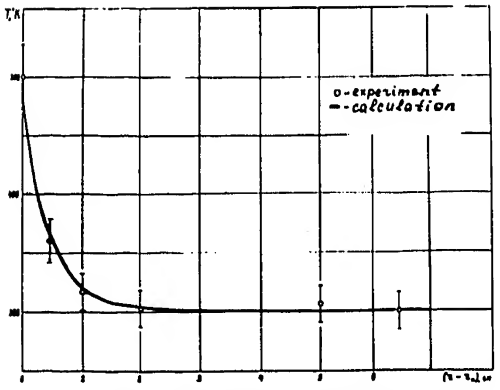

Fig.5. Neutron gas temperature as a function of distance from the source

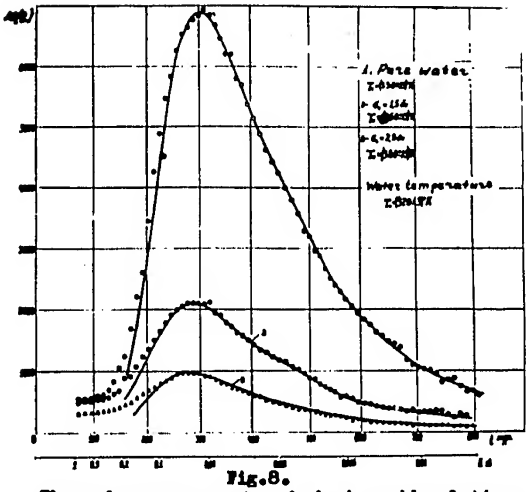

Fig.8.
Thermal neutron spectra in boric acid solutions

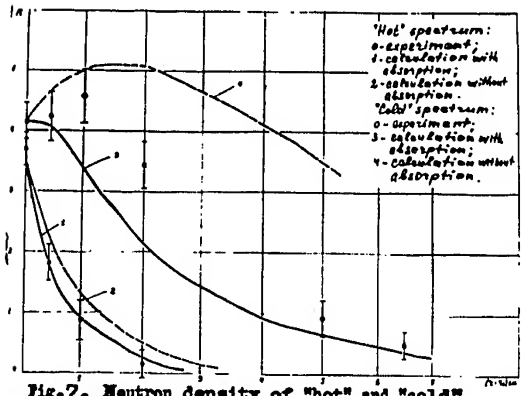

Fig.7. Neutron density of "hot" and "cold" spectrum as a function of distande from the source

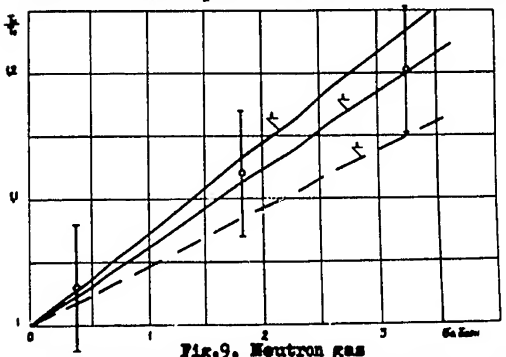

Fig.9. Neutron gas temperature dependence on absorber concentration

366

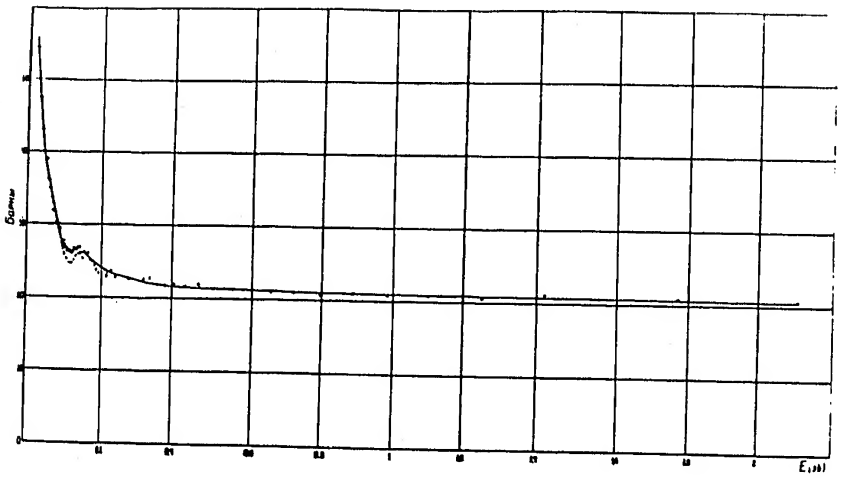

Fig.I0. Lithium-7 hydride total cross-section

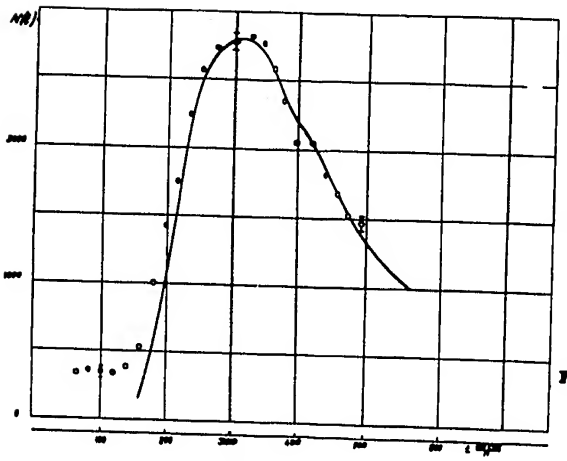

Fig.II.
Thermal neutron spectrum in lithium-7 hydrides $T_0 = 300^{\circ}K$.

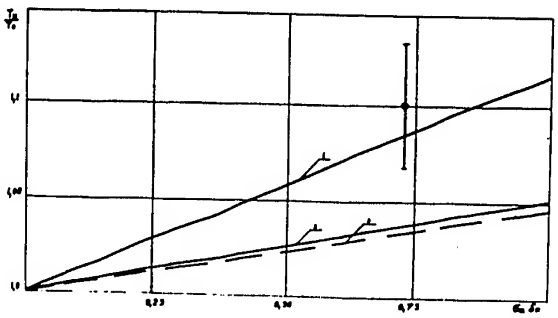

Fig.I2. Neutron gas temperature dependence on absorber concentrations: 1-calculation carried out in [2] for Li-7 hydride; 2-calculation carried out in [2] for water; 3-calculation on the free hydrogen model; o-experimental values for Li-7 hydride

366